Efficient Planning in a Compact Latent Action Space

Zhengyao Jiang
University College London
z.jiang@cs.ucl.ac.uk

Tianjun Zhang
University of California, Berkeley
tianjunz@berkeley.edu

Michael Janner
University of California, Berkeley
janner@berkeley.edu

Yueying Li
Cornell University
yl3469@cornell.edu

Tim Rocktäschel
University College London
tim.rocktaschel@ucl.ac.uk

Edward Grefenstette
University College London & Cohere
e.grefenstette@ucl.ac.uk

Yuandong Tian
Meta AI (FAIR)
yuandong@fb.com

Abstract

While planning-based sequence modelling methods have shown great potential in continuous control, scaling them to high-dimensional state-action sequences remains an open challenge due to the high computational complexity and innate difficulty of planning in high-dimensional spaces. We propose the Trajectory Autoencoding Planner (TAP), a planning-based sequence modelling RL method that scales to high state-action dimensionalities. Using a state-conditional Vector-Quantized Variational Autoencoder (VQ-VAE), TAP models the conditional distribution of the trajectories given the current state. When deployed as an RL agent, TAP avoids planning step-by-step in a high-dimensional continuous action space but instead looks for the optimal latent code sequences by beam search. Unlike $O(D^3)$ complexity of Trajectory Transformer, TAP enjoys constant $O(C)$ planning computational complexity regarding state-action dimensionality D. Our empirical evaluation also shows the increasingly strong performance of TAP with the growing dimensionality. For Adroit robotic hand manipulation tasks with high state and action dimensionality, TAP surpasses existing model-based methods, including TT, with a large margin and also beats strong model-free actor-critic baselines.

1 Introduction

Motivated by the remarkable success of large language generative models (Devlin et al., 2019; Brown et al., 2020), Trajectory Transformer (TT) directly treat the learning of environment dynamics, reward function, value function and policy in model-based reinforcement learning as a single generative sequence modelling problem (Janner et al., 2021). By generating trajectories with a Transformer, TT can accurately plan into more than a hundred future steps in an offline continuous control setting, where conventional one-step models quickly collapses (Janner et al., 2021) due to the compounding error. Since also modelling the behaviour policy that generates the data, TT can easily alleviate the out-of-distribution (OOD) actions problem in the offline RL setting. The accurate sequence modelling ability of Transformer grants TT strong performance in offline model-based continuous control on D4RL (Fu et al., 2020).

However, scaling the Transformer-based trajectory generative model into higher state-action dimensionality is difficult. In order to model the distribution, rather than the expectation, of the trajectories,
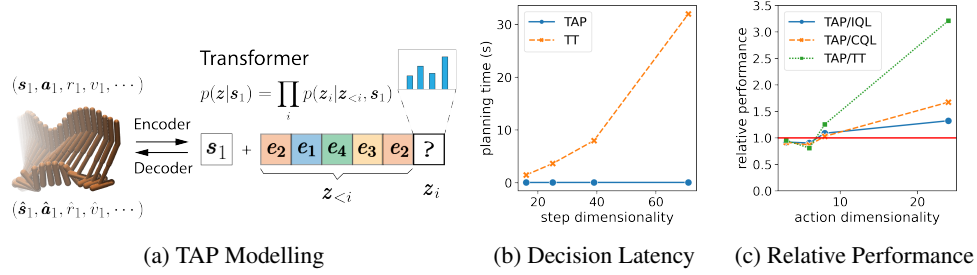
(a) TAP Modelling   (b) Decision Latency   (c) Relative Performance

Figure 1: (a) gives an overview of TAP modelling, where blocks represent the latent codes. (b) shows decision time growth with the dimensionality D. Tests are done on a single GPU. The number of planning steps for (b) is 15 and both models apply a beam search with a beam width of 64 and expansion factor of 4. (c) shows the relative performance between TAP and other baselines when dealing with tasks with increasing action dimensionalities.

one way is to find a discrete representation of the trajectories so that the distribution of the trajectories is categorical. TT discretizes each dimension separately for continuous control tasks and treats each dimension as an individual token. This yields $O(D^2)$ complexity for a forward pass for the state and action dimension D, and $O(D^3)$ single-step sampling cost due to autoregressive sampling of each dimension of the state and action. For tasks with small state/action spaces, such high computational cost and high latency impede real-world deployment, in which frequent replanning is needed. What's more, for most of real-world problems like autonomous driving or household robots, state-action dimensionality can easily blow up with more sensors, even with well-constructed perception or language understanding feature extraction pipelines. This makes the ability to scale up to higher state-action dimensionality even more important. Besides computational cost, a discrete representation of the trajectory will always cause the loss of information, preventing fine-grained control and states prediction.

To tackle high-dimensional continuous control with a trajectory generative model, we consider decoupling the source of stochasticity (discrete random variables) and the representation of the trajectories. Since the marginal distribution of the trajectories is not needed for planning, representing the whole distribution with discrete variables is not necessary. In this paper we propose the Trajectory Autoencoding Planner (TAP), which learned the mapping between the *the possible future trajectories* given the current state and sequence of discrete latent codes, using a state-conditioned Vector Quantised Variational AutoEncoder (VQ-VAE). As illustrated in Figure 1(a), the distribution of these latent codes is then modelled autoregressively with a Transformer, again conditioned on the current state. During inference, instead of sampling the next state/action/reward sequentially, TAP samples latent codes, reconstructs the trajectory via the decoder, and executes the first action in the trajectory with the highest objective score. Every single latent code of TAP corresponds to a branch of the tree of possible trajectories, continuing and forking from the existing trajectory. The forking is caused by different actions sampled from the behaviour policy and the uncertainty of the model. The number of latent variables to model the forking of the trajectories can be much smaller than that of representing the whole trajectories. For example, for a deterministic environment with a deterministic policy, an ideal TAP model should not need extra latent codes to reconstruct the trajectory given a starting state. In practice, TAP uses a single discrete latent variable to model multiple ($L = 3$) steps of transitions, creating a compact latent space for downstream planning. The computational cost of TAP planning is thus $O(C)$ regarding dimensionality D when D is not much larger than the embedding size.

We evaluate TAP extensively in the offline RL setting. Our results on low-dimensional locomotion control tasks show that TAP enjoys competitive performance as strong model-based, model-free actor-critic, and sequence modelling baselines. On tasks with higher dimensionality, TAP not only surpasses model-based methods like TT but also significantly outperforms strong actor-critic baselines. In Figure 1(c), we show how the relative performance between TAP and baselines changes according to the dimensionality of the action space. We can see TAP perform increasingly better when the dimension of actions grows, and it surpass both model-based and model-free methods in higher action dimension control tasks. This can be explained by the innate difficulty of policy op-

2

timization in a high-dimensional action space, which is avoided by TAP since its planning happens in a low-dimensional discrete latent space. At the same time, the sampling and planning of TAP are significantly faster than the Transformer-based generative model: the decision time of TAP meets the requirement of deployment on a real robot (20Hz) (Reed et al., 2022), while TT is much slower and the latency grows along the state-action dimensionality in Figure 1(b).

To sum up, TAP is a planning-based sequence modelling method. Similar to previous sequence modelling methods like TT, the latent structure of the model is not limited to the MDP causal graph, which leads to lower compounding error when predicting multiple steps in future. The main contribution of this work is: 1) We propose to use a state-conditioned VQ-VAE to model the trajectories, which constructs a compact latent action space for downstream planning. 2) We propose to leverage the probability estimation of the generative model to explicitly prevent the agent from choosing actions that either deviate too much from the behaviour policy or lead to low confidence plans. 3) Empirical evaluation in offline RL setting shows TAP efficiently scales up to higher state-action dimensionality, and surpasses previous model-based and model-free methods in high-dimensional continuous control.

2 Background

2.1 Vector Quantised-Variational AutoEncoder

The Vector Quantised-Variational AutoEncoder (VQ-VAE) is a generative model designed based on the Variational AutoEncoder (VAE). There are three components in VQ-VAEs: 1) an encoder network mapping inputs to a collection of discrete latent codes; 2) a decoder that maps latent codes to reconstructed inputs; 3) a learned prior distribution over latent variables. With the prior and the decoder, we can sample data from the VQ-VAE.

In order to represent the input with discrete latent variables, VQ-VAE employs an approach inspired by vector quantization (VQ). The encoder outputs continuous vectors $\boldsymbol{x}_i$ which are not inputted to the decoder directly but used to query a vector in a codebook $\mathbb{R}^{K \times D}$ with K embedding vectors $\boldsymbol{e}_k \in \mathbb{R}^D, k \in 1, 2, 3, ..., K$. The query is done by simply finding the nearest neighbour from K embedding vectors, and the resultant vectors

$$\boldsymbol{z}_i = \boldsymbol{e}_k, \text{where } k = \operatorname{argmin}_j ||\boldsymbol{x}_i - \boldsymbol{e}_j||_2 \tag{1}$$

are input to the decoder. The whole architecture is trained by jointly minimizing the reconstruction error and the distances $||\boldsymbol{x}_i - \boldsymbol{e}_k||_2$ and $||\boldsymbol{z}_i - \boldsymbol{e}_k||_2$. As opposed to vanilla VAEs, the prior of the latent variables are learned by a separate deep model. van den Oord et al. (2017) uses multiple discrete latent variables arranged as a 2D feature map. A pixelCNN is used to model the prior distribution of the latent codes auto-regressively.

3 Method

We use a state-conditional VQ-VAE to model the distribution of trajectories starting from the current state. The encoder, decoder and prior over latent codes are all causal Transformers. In this section, we will provide the model architecture details for TAP and elaborate on the idea of planning in the latent space of the VQ-VAE.

3.1 Conditional Trajectory Generation from Discrete Latents

A trajectory τ consists of a sequence of states, actions, rewards and values:

$$\tau = (\boldsymbol{s}_1, \boldsymbol{a}_1, r_1, v_1, \boldsymbol{s}_2, \boldsymbol{a_2}, r_2, v_2, \ldots, \boldsymbol{s}_T, \boldsymbol{a}_T, r_T, v_T) \tag{2}$$

We concatenate state, action, reward and value [1] in a single step as a feature vector and treat them as a single token for the Transformer encoder and decoder. Transformer-based trajectory generative models (TT and Gato) treat each dimension of the state and action as an individual token. Denoting S as the dimensionality of the state space and A as that of the action space, TT requires $D = S + A + 2$ tokens to model a step of a trajectory. Since the time complexity of the Transformer is $O(N^2)$ for

---

[1]In this work, the value is estimated with Monte Carle estimator, namely, the return-to-go.
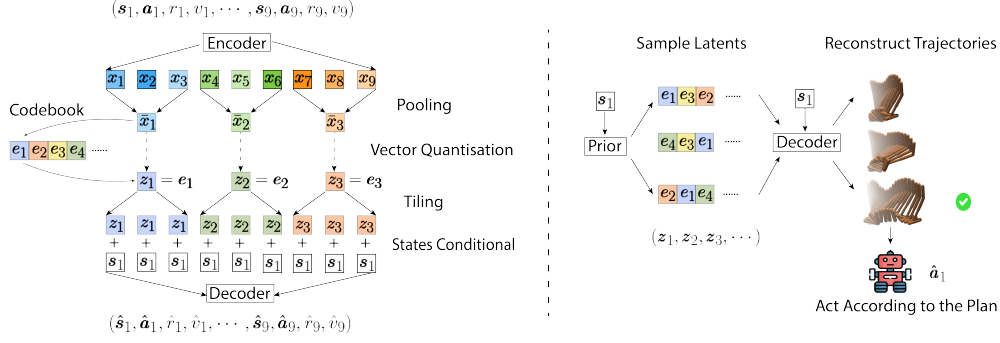
Figure 2: Illustration of training and test time inference process of TAP. The left-hand side shows the training process, highlighting the design of the bottleneck. The right-hand-side figure shows how we generate plans during the test time.

a sequence of length N, the computational cost of TAP is significantly lower especially when the state-action dimensionality is high. Specifically, for a trajectory with T steps, TAP uses T tokens and TT uses TD tokens.

The overall training architecture is illustrated on the left part in Figure 2. The encoder $f_e(\tau) = (\boldsymbol{x}_1, \boldsymbol{x}_2, ..., \boldsymbol{x}_T)$ takes trajectory τ as inputs and returns T feature vectors. We then apply a 1-dimensional max pooling with both kernel size and strides of L, followed by a linear layer. This results in T/L vectors $(\bar{\boldsymbol{x}}_1, \bar{\boldsymbol{x}}_2, ..., \bar{\boldsymbol{x}}_{T/L})$, corresponding to the number of discrete latent variables. After vector quantization in Equation (1), we get embedding vectors for the latent variables $(\boldsymbol{z}_1, \boldsymbol{z}_2, ..., \boldsymbol{z}_{T/L})$. These vectors are then interleaved tiled L times, to match the number of the input/output tokens T. For $L = 3$, this is written as $\mathrm{tile}(\boldsymbol{z}_1, \boldsymbol{z}_2, ..., \boldsymbol{z}_{T/3}) = (\boldsymbol{z}_1, \boldsymbol{z}_1, \boldsymbol{z}_1, \boldsymbol{z}_2, \boldsymbol{z}_2, \boldsymbol{z}_2, ..., \boldsymbol{z}_{T/3}, \boldsymbol{z}_{T/3}, \boldsymbol{z}_{T/3})$

Since we want to leverage the generative model for decision-making rather than generating arbitrary trajectories, it is important to only generate trajectories starting from the current state $\boldsymbol{s}_1$. We made both the auto-encoder and the prior over latent variables conditioned on the first state of the trajectory. The current state can be naturally incorporated into the trajectory for the encoder. For the decoder f_d, we concatenate the state and embedding vector for the codes and apply a linear projection to match the dimensionality of the feature vector. We denote the operator that blends state information to the latent embeddings as $\mathrm{mixing}(\boldsymbol{z}_1, \boldsymbol{z}_2, ..., \boldsymbol{z}_T, \boldsymbol{s}_1)$. After adding the positional embedding, the encoder then reconstructs the trajectory $(\hat{\boldsymbol{s}}_1, \hat{\boldsymbol{a}}_1, \hat{r}_1, \hat{v}_1, \hat{\boldsymbol{s}}_2, \hat{\boldsymbol{a}}_2, \hat{r}_2, \hat{v}_2, ..., \hat{\boldsymbol{s}}_T, \hat{\boldsymbol{a}}_T, \hat{r}_T, \hat{v}_T)$. The reconstruction loss is the mean squared error over input trajectories and reconstructed ones.

With the autoencoder in place, we use a Transformer to autoregressively model the distribution of the latent codes given the initial state $\boldsymbol{s}_1$. The state information is also blended into the architecture by the concatenation of token embeddings. We denote the state-conditional prior model as $p(\boldsymbol{z}_i|\boldsymbol{z}_{<i}, \boldsymbol{s}) = p(\boldsymbol{z}_i|\boldsymbol{s}_1, \boldsymbol{z}_1, \boldsymbol{z}_2, ..., \boldsymbol{z}_{i-1})$.

Interpret Latent Codes A key design choice we made is to let the decoder, not only the prior of latents, be conditioned on the current state. Such a design leads to a compact latent action space that enables efficient planning. Without the state as input, the decoder must reconstruct the whole trajectory relying solely on the latent codes, so the latent codes contain information about the whole trajectory segments (states, actions, rewards, values). In other words, latent codes will be a discrete representation of the trajectory, where a latent codes sequence can be decoded into a unique trajectory. On the other hand, conditioned on the current state, the latent codes only need to carry information about how the future trajectories branch from the existing trajectory. Every L step, a branch of the trajectory will fork into K possible futures. Each of the latent codes corresponds to a branch of this tree of possible future trajectories, where the root node is the current state. The forking can be caused by the uncertainty of the dynamics model or by the stochasticity of the behaviour policy. The number of latent codes needed to reconstruct a trajectory given a starting state will reduce as long as the model knows more about the dynamics of the environment and the behaviour policy. Assume a trajectory distribution $p(\tau|\boldsymbol{s}_1; \mu)$ with behaviour policy μ has deterministic Markovian

4

transition dynamics, and the model has recovered the true dynamics. The probability of a valid trajectory that fit the dynamics can be expressed as $p(\tau|\boldsymbol{s}_1; \mu) = \prod_{i=1}^{T} \mu(\boldsymbol{a}_i|\boldsymbol{s}_i)$. So the discrete latent variables only need to approximate the distribution of the behaviour policy, where latent codes correspond to grouped components of the behaviour policy. Note that the policy is not only grouped in a single step but also across multiple steps. Intuitively, the latent codes can then be interpreted as state-conditioned options (Sutton et al., 1999), learning by decomposing the behaviour policy into a weighted sum of sub-policies. The number of grouped policy components of the behaviour policy can be much less than the dimensionalities needed to represent the whole trajectory. As we will show in Section 4.3, the $L = 3$ or $L = 4$ gives an optimal performance of TAP on D4RL tasks, which means 3 steps of the transitions with up to hundreds of dimensions can be expressed with a single discrete latent variable, with $K = 512$ bins. In contrast, the discrete representation of the trajectory used in TT will allocate LD discrete codes to describe the same number of transitions. This means TAP has a smaller and more compact latent space for downstream planning.

3.2 Planning in the Latent Space

We now describe how to plan with a TAP model. We denote the parts of the bottleneck after vector quantisation and the decoder as a monolithic mapping:

$$h(\boldsymbol{s}_1, \boldsymbol{z}_1, \boldsymbol{z}_2, ..., \boldsymbol{z}_{T/L}) = f_d(\text{mixing}(\text{tile}(\boldsymbol{z}_1, \boldsymbol{z}_2, ..., \boldsymbol{z}_{T/L}), \boldsymbol{s}_1)) \quad (3)$$

that turns the current state and latent embeddings into a trajectory. We will select the best trajectory as our plan according to the score function g. One part of the score function is the predicted return-to-go following the action sequences in the decoded trajectory, coloured red in Equation (4). On the other hand, only optimizing for the return will face the problem of offline RL with out-of-distribution (OOD) actions (Kumar et al., 2019). For TAP, if an OOD latent code sequence is sampled then it is more likely the model will give an inaccurate prediction both in terms of future states and also future rewards and values. These inaccuracies can lead to over-optimistic return estimation for trajectories. One way to reduce the chance to get an OOD trajectory is to sample with the learned prior, which is the default behaviour of VQ-VAE. However, when we apply an optimizer to find a trajectory that has a higher return, the optimizer is implicitly encouraged to find these over-optimistic trajectories. We address this problem by adding a penalty if the prior probability of a trajectory is lower than a threshold $\beta^{T/L}$, coloured blue, giving the following objective function:

$$g(\boldsymbol{s}_1, \boldsymbol{z}_1, \boldsymbol{z}_2, ..., \boldsymbol{z}_{T/L}) = \sum_i \gamma^i \hat{r}_i + \gamma^T \hat{v}_T + \alpha \ln\left(\text{clip}(p(\boldsymbol{z}_1, \boldsymbol{z}_2, ..., \boldsymbol{z}_{T/L}|\boldsymbol{s}_1), 0, \beta^{T/L})\right) \quad (4)$$

where α is the weight of the penalty and $\hat{r}_i$ and $\hat{v}_T$ are estimated reward and value from decoded trajectory $(\hat{\boldsymbol{s}}_1, \hat{\boldsymbol{a}}_1, \hat{r}_1, \hat{v}_1, \hat{\boldsymbol{s}}_2, \hat{\boldsymbol{a}}_2, \hat{r}_2, \hat{v}_2, ..., \hat{\boldsymbol{s}}_T, \hat{\boldsymbol{a}}_T, \hat{r}_T, \hat{v}_T) = h(\boldsymbol{s}_1, \boldsymbol{z}_1, \boldsymbol{z}_2, ..., \boldsymbol{z}_{T/L})$. We set α to be a large number compared to the range of the discounted returns in order to encourage the more likely trajectory to be selected if the prior probability is lower than the threshold. However, for the trajectories whose prior probability is higher than the threshold, the OOD penalty will not be activated and the trajectories with the higher return will always be selected.

Vanilla Sampling   The most straightforward way to search in the latent space of TAP is to sample according to the prior distribution and select the trajectory that gives the best return. Conditioned on current state $\boldsymbol{s}_1$, we can sample N latent variables sequences autoregressively according to the prior model: $(\boldsymbol{z}_1, \boldsymbol{z}_2, ..., \boldsymbol{z}_{T/L})_n \sim p(\boldsymbol{z}_1, \boldsymbol{z}_2, ..., \boldsymbol{z}_{T/L}|\boldsymbol{s}_1)$ where $n \in 1, 2, 3, ..., N$. These latent variable sequences will be then turned into trajectories τ_n where $n \in 1, 2, 3, ..., N$ so that we can take the optimal one according to the objective function Equation (4). This naive approach works well when the overall length of the trajectory is small since the discrete latent space is significantly smaller than the raw action space. However, such an approach will quickly degenerate when the planning horizon grows.

Beam Search in the Latent Space   Since our encoder and decoder are causal transformers and latent variables are arranged in temporal order, we can partially decode the first nL steps of the trajectory $\tau_{<nL+1}$ with the first n latent codes $z_{<n+1}$. With that property in place, it is possible to apply more advanced planning that exploits the information of the partially reconstructed trajectories, rather than direct sampling according to the prior. An easy way to incorporate both the information of the prior distribution and partially decoded trajectories is beam search. In general,

each step of TAP beam search with beam width B and expansion factor E samples E new latents conditioned on each of the B context latents. The top B latents in terms of decoded returns are preserved and kept as context. The pseudocode of the TAP beam search is shown in Algorithm 1. In practice, we find TAP with beam search is usually computationally more efficient because it can find the optimal trajectory with fewer queries to the generative model.

Algorithm 1 TAP Beam Search

Input: Current state $\boldsymbol{s}$, sequence length T, beam width B, expansion factor E, prior model p and decoding function h

1: Sample initial context latents $Z_1 = \{\boldsymbol{z}_1^{(n)} | \boldsymbol{z}_1^{(n)} \sim p(\boldsymbol{z}|\boldsymbol{s}), n \leq BE\}$
2: **for** $t = 2$ to T **do**
3:      **for** $b = 1$ to B **do**
4:          Expand the beam $\mathcal{C}_t \leftarrow \{(\boldsymbol{z}_{<t})^{(b)} \circ \boldsymbol{z}_e | \boldsymbol{z}_e \sim p(\boldsymbol{z}_t|\boldsymbol{z}_{<t}^{(b)}, \boldsymbol{s}), e \leq E\}$
5:      **end for**
6:      Decode Trajectories $\mathcal{T}_t \leftarrow \{\tau | \tau = h(\boldsymbol{z}_{<t+1}, \boldsymbol{s}), \boldsymbol{z}_{<t+1} \in \mathcal{C}_t\}$
7:      Get top B trajectories according to return
8:      Set corresponding latent sequences to be Z_t
9: **end for**
10: **return** best trajectory in $\mathcal{T}_T$

---

4 Experiments

The empirical evaluation of TAP consists of three sets of tasks from D4RL(Fu et al., 2020): gym locomotion control, AntMaze and Adroit. Gym locomotion control serves as a proof of concept in the low-dimensional domain to test if TAP can accurately reconstruct trajectories that can be used for downstream control. We then test TAP on Adroit, which has high state and action dimensionality, which TT struggles to handle because of the long token sequence length. Finally, we also test TAP on AntMaze, a sparse-reward continuous-control problem. TAP achieve a similar performance as TT on AntMaze, surpassing model-free methods, where the details can be found in Appendix E.

4.1 Setup

We set the number of the steps associated with the latent variable to be $L = 3$ and each latent variable has $K = 512$ candidate values. The planning horizon will be 15 for gym-locomotion and 24 for adroit. This means the planning process only needs to optimize in a 5 or 8-dimensional discrete space, with the guide of the learned prior. We use beam search to produce all of our results, which has lower decision latency compared to direct sampling with similar performance but a larger sample size. Other hyperparameters including architectures can be found in the Appendix. We test each task with 5 training seeds, each evaluated for 20 episodes. Following the evaluation protocol of TT and IQL, we use the v2 version of the datasets for locomotion control and v0 for the other tasks.

4.2 Results

Our first set of empirical evaluations is on gym locomotion control tasks. In this suite of tasks, TAP managed to be competitive against the strong baselines on average. On the other hand, the performance of model-based baselines on the adroit tasks is much worse than the case on tasks with lower state and action dimensionality, showing inferior dimension scalability. Model-free actor-critic methods (CQL, IQL) used to be significantly stronger than model-free ones (MOPO, TT) on adroit, and TAP becomes the first model-based approach that surpasses model-free methods. Notably, given the higher state and action dimensionality, the computational cost and inference latency of TT on Adroit is very high (30 seconds needs to make one step of decision).

To show how the relative performance between TAP and baselines vary along with action dimensions, we averaged up relative performance on tasks of the same action dimensionality and plotted them in Figure 1(c). [2] The x-axis is the action dimensionality of the tasks and the horizontal red line

---

[2]We didn't include expert datasets for adroit when computing average since the common protocol for gym locomotion evaluation also doesn't include expert datasets and the IQL paper didn't report these scores.

shows the relative performance of 1, meaning two methods achieve the same score. We can see that TAP scales better in terms of decision latency compared to TT. Also, TAP shows better performance for tasks with higher action dimensionality, compared to both TT and other model-free actor-critic methods (CQL/IQL). This can be explained by the increasing difficulty of policy optimization in larger action space due to the curse of dimensionality. On the other hand, TAP does the optimization in a compact latent space with a handful of discrete latent variables. Notably, the performance of actor-critic methods provides a context but they focus on policy improvement and value estimation, which is orthogonal to the contribution of TAP and TT in modelling the trajectory distribution. Combining the low-variance off-policy value estimation with an accurate model can potentially lead to even better performance as shown in the antmaze experiments of TT (Janner et al., 2021).

Table 1: Locomotion control results. Numbers are normalised scores following the protocol of Fu et al. (2020).

Dataset	Environment	BC	CQL	IQL	DT	MOReL	TT	TAP (Ours)
Medium-Expert	HalfCheetah	59.9	91.6	86.7	86.8	53.3	**95.0**	91.8 ±0.8
Medium-Expert	Hopper	79.6	105.4	91.5	107.6	108.7	**110.0**	105.5 ±1.7
Medium-Expert	Walker2d	36.6	108.8	**109.6**	108.1	95.6	101.9	107.4 ±0.9
Medium-Expert	Ant	114.2	115.8	125.6	122.3	−	116.1	**128.8** ±2.4
Medium	HalfCheetah	43.1	44.4	**47.4**	42.6	42.1	46.9	45.0 ±0.1
Medium	Hopper	63.9	58.0	66.3	67.6	**95.4**	61.1	63.4 ±1.4
Medium	Walker2d	77.3	72.5	78.3	74.0	77.8	**79.0**	64.9 ±2.1
Medium	Ant	92.1	90.5	**102.3**	94.2	−	83.1	92.0 ±2.4
Medium-Replay	HalfCheetah	4.3	**45.5**	44.2	36.6	40.2	41.9	40.8 ±0.6
Medium-Replay	Hopper	27.6	**95.0**	94.7	82.7	93.6	91.5	87.3 ±2.3
Medium-Replay	Walker2d	36.9	77.2	73.9	66.6	49.8	**82.6**	66.8 ±3.1
Medium-Replay	Ant	89.2	93.9	88.8	88.7	−	77.0	**96.7** ±1.4
Mean		60.4	83.2	84.1	81.5	−	82.2	82.5

Table 2: Adroit robotic hand control results.

Dataset	Environment	BC	CQL	IQL	MOPO	Opt-MOPO	TT	TAP (Ours)
Human	Pen	34.4	37.5	71.5	6.2	19.0	36.4	**76.5** ±8.5
Human	Hammer	1.5	**4.4**	1.4	0.2	0.5	0.8	1.4 ±0.1
Human	Door	0.5	**9.9**	4.3	−	−	0.1	8.8 ±1.1
Human	Relocate	0.0	0.2	0.1	−	−	0.0	0.2 ±0.1
Cloned	Pen	56.9	39.2	37.3	6.2	23.0	11.4	**57.4** ±8.7
Cloned	Hammer	0.8	2.1	2.1	0.2	**5.2**	0.5	1.2 ±0.1
Cloned	Door	−0.1	0.4	1.6	−	−	−0.1	**11.7** ±1.5
Cloned	Relocate	−0.1	−0.1	−0.2	−	−	−0.1	−0.2 ±0.0
Expert	Pen	85.1	107.0	−	15.1	50.6	72.0	**127.4** ±7.7
Expert	Hammer	125.6	86.7	−	6.2	23.3	15.5	**127.6** ±1.7
Expert	Door	34.9	101.5	−	−	−	94.1	**104.8** ±0.8
Expert	Relocate	101.3	95.0	−	−	−	10.3	**105.8** ±2.7
Mean (without Expert)		11.7	11.7	14.8	−	−	6.1	**19.6**
Mean (all settings)		36.7	40.3	−	−	−	20.1	**51.9**

4.3 Analysis

TAP is a novel sequence modelling RL method which involves several designs that can potentially be transferred to other model-based or offline RL methods. In order to provide a better insight into these design choices, we provide analyses here, together with ablations of common hyper-parameters like planning horizon. In Figure 3, we showed a summary of the results of ablation studies on gym locomotion tasks, the full results for more hyper-parameters and scores for each individual task can be found in the Appendix.
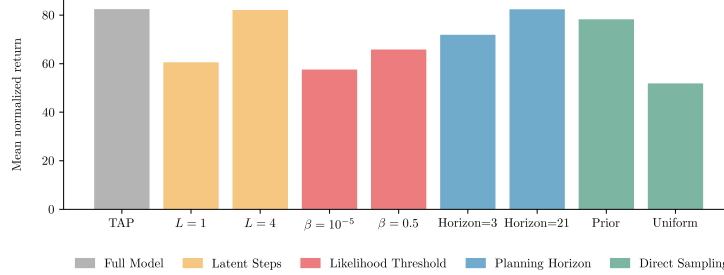
Figure 3: Results of ablation studies, where the height of the bar is the mean normalised scores on gym locomotion control tasks.

Latent Steps   An obvious feature of TAP is the planning is not unrolled step-by-step. Whenever a single latent code is sampled, L steps of transitions that continue the previous trajectory can be decoded. This can obviously increase the efficiency of planning since the number of steps of unrolling is reduced to $\frac{1}{L}$ therefore the search space is exponentially reduced in size. However, it is unclear how such a design will affect the decision-making performance of the method. We thus tested TAP with different latent step L, namely, the number of steps associated with a latent variable. As shown in the yellow bars in Figure 3, it turns out that reducing the latent step to 1 will significantly undermine the performance of TAP. We hypothesize that the performance drop is related to the overfitting of the VQ-VAE since we observe the reduced latent step leads to a higher estimated return and also a higher prediction error. On the other hand, further increasing the latent length to 4 will not bring an extra performance boost.

OOD Penalty   By varying the threshold for probability clipping (β), we also tested the benefits of OOD penalty and return estimations in the objective function Equation (4). When $\beta = 10^{-5}$, the OOD penalty is not likely to be activated and TAP will try to maximize the estimated return only. When $\beta = 0.5$, the OOD penalty will always be activated and encourage the agent to choose the most likely trajectory, namely, imitating the behaviour policy. In these two cases, the performance of the TAP agent drops 30.2% and 20.2% respectively. This shows solely optimizing the return or prior probability leads to suboptimal performance, so both ingredients are necessary for the objective function. Nevertheless, it is worth noting that besides these extreme values, the performance of TAP is robust to a wide range of choices of β, ranging from 0.002 to 0.1, as shown in Table 4.

Planning Horizon   We also tested how the planning horizon will affect the performance of TAP. Surprisingly, TAP is not very sensitive to the planning horizon, and managed to achieve a mean score of 71.9 (-12.9%) by simply expanding a single latent variable, thus doing 3 steps of planning. Notably, this conclusion might be bound to the tasks, as dense-reward locomotion control may need less reasoning than tasks like board games.

Beam Search   Another ablation is about whether structured search (beam search) is helpful, compared to direct sampling from the latent space. We tested the TAP agent with a direct sampling of 2048 trajectories according to the prior. As shown in the green bar with "Prior" label in Figure 3, it turns out beam search still performs slightly better and its decision latency is also lower because the beam width we used (64) is much lower than the number of samples needed for direct sampling (2048). On the other hand, we believe the fact that even direct sampling can generate decent plans for TAP shows the latent space for TAP is compact and can be used for efficient planning.

Sampling from Prior   When TAP doing beam search or direct sampling, the latent codes are sampled from the learned prior distribution rather than uniformly. Such a design is straightforward for Vanilla VQ-VAE since the objective, in that case, is to sample from the dataset distribution. However, for the case of RL, the aim is a bit different since we want to find an optimal trajectory in terms of return with an OOD penalty. We therefore also tested direct sampling where the latent codes are uniformly sampled, whose performance is illustrated as a green bar with a "Uniform" label in Figure 3. It turns out sampling according to the uniform distribution will largely (-37.9%) damage the performance of the agent, even with an OOD penalty. To further investigate the role of

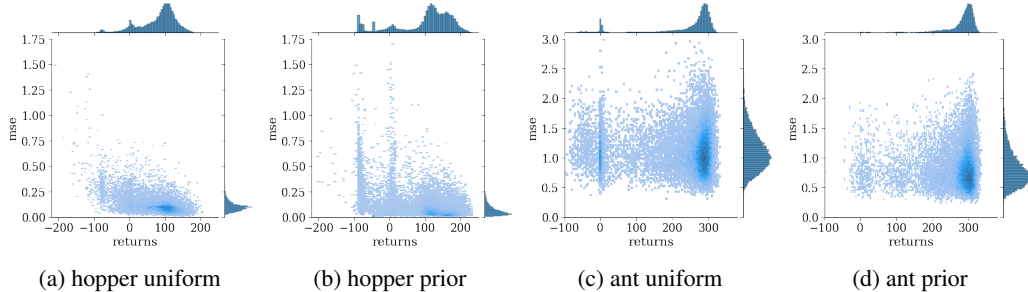(a) hopper uniform   (b) hopper prior   (c) ant uniform   (d) ant prior

Figure 4: Distribution of trajectory returns and state prediction mean-squared errors. The dataset for the hopper is medium-replay and that for ant is medium.

sampling from the prior, in Figure 4 we visualize the distribution of trajectories modelled by TAP in two locomotion tasks. We sampled 2048 trajectories either uniformly or according to the prior in the first step of the 10 evaluation episodes. The x-axis of the plots is predicted returns by the agents. The y-axis shows the state's prediction mean-squared error (MSE), where the ground truth is given by the simulator following the action sequences of the predicted trajectories. Sampling from the prior does not damage the diversity of the sampled trajectories in terms of the variance of returns. On the other hand, the expected MSE is reduced in both hopper and ant cases. This means that by sampling from the prior, we can get a higher quality of trajectory samples.

4.4 Decision Latency

Besides the computational complexity of the forward pass and sampling, we also tested how exactly the computational costs and decision latency of TT and TAP grow along with the state-action dimensionality of the tasks. Tests are done on a platform with i5 12900K CPU and a single RTX3090 GPU. We fix the planning horizon to be 15 (default planning horizon for TT) and test their decision time on hopper ($D = 14$), halfcheetah ($D = 23$), ant ($D = 37$) and adroit-pen ($D = 71$). Even for the task with the lowest dimensionality, TT needs 1.5 seconds to make a decision and the latency grows to 32 seconds when dealing with adroit. On the other hand, TAP manages to make a decision within 0.05 seconds and meets the real-world robotics deployment criterion proposed by Reed et al. (2022). Moreover, the latency almost keeps the same for different dimensionality, making it computationally feasible to be applied to high-dimensional control tasks.

5 Related Work

RL as Sequence modelling Problems   TAP follows a recent line of work that treats RL as a sequence modelling problem (Chen et al., 2021a; Janner et al., 2021; Zheng et al., 2022). They use GPT-2 (Radford et al., 2019) style Transformers (Vaswani et al., 2017) to model the whole trajectory of states, actions, rewards and values, and turn the prediction ability into a policy. The two orthogonal design choices for these sequence modelling methods are 1) how to model the trajectories and 2) how to turn the model into a policy. On the modelling side, Decision Transformer (DT) (Chen et al., 2021a) only models the expected action while Trajectory Transformer (TT) (Janner et al., 2021) and Gato (Reed et al., 2022) model the full distribution of trajectories by discretizing the continuous state/action spaces. During acting, DT applies an Upside Down RL (Schmidhuber, 2019) approach to predict actions conditioned on rewards. We regard DT as a less-relevant work because such a model is history- and return-conditioned policy rather than a trajectory generative model. Gato applies an imitation learning approach and sample actions conditioned on the historical trajectory. TT, in the offline RL setting, applies planning in order to find the best trajectory that gives the highest return.

A concurrent work of ours is Diffusser (Janner et al., 2022), which is also a trajectory generative model but based on the diffusion model. The planning of Diffuser is based on classifier-guided sampling and image inpainting. The planning of Diffuser is on trajectory level rather than dimension level and thus also has better scalability in terms of state-dimensionality and planning horizon. However, similar to the diffusion model for image generation, the time needed to generate a sample with

the diffuser is long. While it is possible to speed up the sampling by reusing previous plans, it comes with the price of losing performance (Janner et al., 2022). In contrast, without additional techniques for speeding up planning, the decision frequency of TAP is ready for real-time decision-making problems.

Trajectory Generation   Chen et al. (2021b) use VAEs and GANs to generate trajectories but not for downstream control. Lu et al. (2019) use VAEs to model expert data and generates varied data for imitation learning. In robotics literature, Barbié et al. (2019) use conditional VAE to generate trajectories as initial guesses for conventional motion planners. These trajectory generation models are usually only modelling states and actions, some of them only states. This is different from the RL sequence modelling approaches where rewards and values are also modelled. With reward and values modelling, we can construct policies that can go beyond behaviour policy as shown in our experiments. Another difference between our work and the prior VAE trajectory generation model is we do optimization (planning) in the latent space.

Model-based RL   TAP is a member of model-based RL methods (Sutton, 1990; Silver et al., 2008; Fairbank, 2008; Deisenroth and Rasmussen, 2011; Lampe and Riedmiller, 2014; Heess et al., 2015; Wang and Ba, 2020; Schrittwieser et al., 2020; Amos et al., 2021; Hafner et al., 2021) since it learns to predict into future and turns that prediction ability into a policy. The model these methods learned, however, are all dynamics models of an MDP, which takes current state and action as inputs and returns the (distribution of) future states and rewards. TAP is different from these conventional model-based methods since the TAP decoder does not strictly follow the MDP causal structure but takes latent variables and the current state as inputs, returning a whole trajectory. These latent variables act as a learned latent action space which is compact and allows efficient planning.

Planning with State Latent Space   Hafner et al. (2019) proposed PlaNet that models the dynamics with the Recurrent State Space Model and plans in the continuous state latent space with Model Predictive Control. Ozair et al. (2021) trains a VQVAE to turn the observation into the discrete latent space and plan with Monte Carlo Tree Search. Our work did not learn a representation of states or even a representation of the trajectory but the latent space of possible completion of existing trajectories. The information needed to generate a completion trajectory is much less than generate an arbitrary trajectory, which leads to a smaller latent space. Each latent variable corresponds to a possible completion and forms a compact latent action space for planning, which is different from the latent state space.

Planning in the Action Latent Space   Wang et al. (2020); Yang et al. (2021) proposed to learn representations of actions on-the-fly for black-box optimization and path planning setting. While relevant on a high level, these works usually operate in continuous latent space leading to different planning procedures and more importantly the environment dynamics are assumed to be known in advance. TAP is the first one that applies a similar idea to the RL setting where the true dynamics of the environment are unknown so that we learn the dynamics model and encoder/decoder of the planning action space jointly with a VQ-VAE.

Offline RL   In this paper, TAP is tested in an offline RL setting (Ernst et al., 2005) where we are not allowed to use online experience to improve our policy. A major challenge of offline RL is to prevent out-of-distribution (OOD) actions to be chosen by the learned policy, so that the inaccuracy of the value function and the model will not be exploited. To address that, all kinds of techniques to introduce conservativeness are proposed (Kumar et al., 2020; Fujimoto and Gu, 2021; Lu et al., 2022; Kostrikov et al., 2022; Kidambi et al., 2020). TAP can naturally prevent the OOD actions or in general OOD sequences because it models trajectories generated by behaviour policy. This means all the plans sampled from the model should be in distribution. To further discourage OOD trajectories to be selected as the plan, we add an OOD penalty given by the learned prior at the planning time.

Hierarchical RL   One conceptually relevant work to ours is (Co-Reyes et al., 2018), where they use a VAE to project the state sequences into continuous latent variables and have policies conditioned on not only the current state but also the latent variable. Differing from our work that models actions, states, rewards and values jointly with a unified Transformer, they learned a state decoder and a step-by-step policy decoder that is trained separately. The policy decoder in their case has to

be trained with a conventional RL algorithm with approximate gradients, whereas TAP follows the sequence modelling approaches and is trained fully with (self-)supervised signals. Our work is also remotely related to RL in the option framework (Sutton et al., 1999; Stolle and Precup, 2002; Bacon et al., 2017) since both the latent codes of TAP and option introduced the temporal abstraction of the RL trajectories.

6 Limitations

One of the limitations of TAP is that it cannot distinguish between the uncertainty coming from the behaviour policy and the uncertainty from the environment dynamics. This might cause over-optimistic behaviours if the environment has intrinsic stochasticity since we are searching for trajectories with a higher return. This problem only exists in the offline RL setting; in imitation learning, it is possible to directly sample from the latent code without optimization. Another potential disadvantage compared to Transformer-based generative models is the loss of fine-grained control of the generated trajectories. For example, we cannot easily propose an arbitrary action for conditioning the model's trajectory samples. Also, as a planning-based method with Transformers in the architecture, the decision latency is still inevitable longer than model-free methods as they only need a single policy network inference. While we argue that the computational complexity regarding the state-action dimensionality is the same as model-free methods.

References

Amos, B., Stanton, S., Yarats, D., and Wilson, A. G. (2021). On the model-based stochastic value gradient for continuous reinforcement learning. In Jadbabaie, A., Lygeros, J., Pappas, G. J., Parrilo, P. A., Recht, B., Tomlin, C. J., and Zeilinger, M. N., editors, *Proceedings of the 3rd Annual Conference on Learning for Dynamics and Control, L4DC 2021, 7-8 June 2021, Virtual Event, Switzerland*, volume 144 of *Proceedings of Machine Learning Research*, pages 6–20. PMLR.

Bacon, P., Harb, J., and Precup, D. (2017). The option-critic architecture. In Singh, S. and Markovitch, S., editors, *Proceedings of the Thirty-First AAAI Conference on Artificial Intelligence, February 4-9, 2017, San Francisco, California, USA*, pages 1726–1734. AAAI Press.

Barbié, T., Nishio, T., and Nishida, T. (2019). Trajectory prediction with a conditional variational autoencoder. *J. Robotics Mechatronics*, 31(3):493–499.

Brown, T. B., Mann, B., Ryder, N., Subbiah, M., Kaplan, J., Dhariwal, P., Neelakantan, A., Shyam, P., Sastry, G., Askell, A., Agarwal, S., Herbert-Voss, A., Krueger, G., Henighan, T., Child, R., Ramesh, A., Ziegler, D. M., Wu, J., Winter, C., Hesse, C., Chen, M., Sigler, E., Litwin, M., Gray, S., Chess, B., Clark, J., Berner, C., McCandlish, S., Radford, A., Sutskever, I., and Amodei, D. (2020). Language models are few-shot learners. In Larochelle, H., Ranzato, M., Hadsell, R., Balcan, M., and Lin, H., editors, *Advances in Neural Information Processing Systems 33: Annual Conference on Neural Information Processing Systems 2020, NeurIPS 2020, December 6-12, 2020, virtual*.

Chen, L., Lu, K., Rajeswaran, A., Lee, K., Grover, A., Laskin, M., Abbeel, P., Srinivas, A., and Mordatch, I. (2021a). Decision transformer: Reinforcement learning via sequence modeling. In Beygelzimer, A., Dauphin, Y., Liang, P., and Vaughan, J. W., editors, *Advances in Neural Information Processing Systems*.

Chen, X., Xu, J., Zhou, R., Chen, W., Fang, J., and Liu, C. (2021b). Trajvae: A variational autoencoder model for trajectory generation. *Neurocomputing*, 428:332–339.

Co-Reyes, J. D., Liu, Y., Gupta, A., Eysenbach, B., Abbeel, P., and Levine, S. (2018). Self-consistent trajectory autoencoder: Hierarchical reinforcement learning with trajectory embeddings. In Dy, J. G. and Krause, A., editors, *Proceedings of the 35th International Conference on Machine Learning, ICML 2018, Stockholmsmässan, Stockholm, Sweden, July 10-15, 2018*, volume 80 of *Proceedings of Machine Learning Research*, pages 1008–1017. PMLR.

Deisenroth, M. P. and Rasmussen, C. E. (2011). PILCO: A model-based and data-efficient approach to policy search. In Getoor, L. and Scheffer, T., editors, *Proceedings of the 28th International Conference on Machine Learning, ICML 2011, Bellevue, Washington, USA, June 28 - July 2, 2011*, pages 465–472. Omnipress.

Devlin, J., Chang, M., Lee, K., and Toutanova, K. (2019). BERT: pre-training of deep bidirectional transformers for language understanding. In Burstein, J., Doran, C., and Solorio, T., editors, *Proceedings of the 2019 Conference of the North American Chapter of the Association for Computational Linguistics: Human Language Technologies, NAACL-HLT 2019, Minneapolis, MN, USA, June 2-7, 2019, Volume 1 (Long and Short Papers)*, pages 4171–4186. Association for Computational Linguistics.

Ernst, D., Geurts, P., and Wehenkel, L. (2005). Tree-based batch mode reinforcement learning. *J. Mach. Learn. Res.*, 6:503–556.

Fairbank, M. (2008). Reinforcement learning by value gradients. *CoRR*, abs/0803.3539.

Fu, J., Kumar, A., Nachum, O., Tucker, G., and Levine, S. (2020). D4RL: datasets for deep data-driven reinforcement learning. *CoRR*, abs/2004.07219.

Fujimoto, S. and Gu, S. (2021). A minimalist approach to offline reinforcement learning. In Beygelzimer, A., Dauphin, Y., Liang, P., and Vaughan, J. W., editors, *Advances in Neural Information Processing Systems*.

Hafner, D., Lillicrap, T. P., Fischer, I., Villegas, R., Ha, D., Lee, H., and Davidson, J. (2019). Learning latent dynamics for planning from pixels. In Chaudhuri, K. and Salakhutdinov, R., editors, *Proceedings of the 36th International Conference on Machine Learning, ICML 2019, 9-15 June 2019, Long Beach, California, USA*, volume 97 of *Proceedings of Machine Learning Research*, pages 2555–2565. PMLR.

Hafner, D., Lillicrap, T. P., Norouzi, M., and Ba, J. (2021). Mastering atari with discrete world models. In *9th International Conference on Learning Representations, ICLR 2021, Virtual Event, Austria, May 3-7, 2021*. OpenReview.net.

Heess, N., Wayne, G., Silver, D., Lillicrap, T. P., Erez, T., and Tassa, Y. (2015). Learning continuous control policies by stochastic value gradients. In Cortes, C., Lawrence, N. D., Lee, D. D., Sugiyama, M., and Garnett, R., editors, *Advances in Neural Information Processing Systems 28: Annual Conference on Neural Information Processing Systems 2015, December 7-12, 2015, Montreal, Quebec, Canada*, pages 2944–2952.

Janner, M., Du, Y., Tenenbaum, J., and Levine, S. (2022). Planning with diffusion for flexible behavior synthesis. In *International Conference on Machine Learning*.

Janner, M., Li, Q., and Levine, S. (2021). Offline reinforcement learning as one big sequence modeling problem. In Beygelzimer, A., Dauphin, Y., Liang, P., and Vaughan, J. W., editors, *Advances in Neural Information Processing Systems*.

Kidambi, R., Rajeswaran, A., Netrapalli, P., and Joachims, T. (2020). Morel: Model-based offline reinforcement learning. In Larochelle, H., Ranzato, M., Hadsell, R., Balcan, M., and Lin, H., editors, *Advances in Neural Information Processing Systems 33: Annual Conference on Neural Information Processing Systems 2020, NeurIPS 2020, December 6-12, 2020, virtual*.

Kostrikov, I., Nair, A., and Levine, S. (2022). Offline reinforcement learning with implicit q-learning. In *International Conference on Learning Representations*.

Kumar, A., Fu, J., Tucker, G., and Levine, S. (2019). Stabilizing off-policy q-learning via bootstrapping error reduction.

Kumar, A., Zhou, A., Tucker, G., and Levine, S. (2020). Conservative q-learning for offline reinforcement learning. In Larochelle, H., Ranzato, M., Hadsell, R., Balcan, M., and Lin, H., editors, *Advances in Neural Information Processing Systems 33: Annual Conference on Neural Information Processing Systems 2020, NeurIPS 2020, December 6-12, 2020, virtual*.

Lampe, T. and Riedmiller, M. A. (2014). Approximate model-assisted neural fitted q-iteration. In *2014 International Joint Conference on Neural Networks, IJCNN 2014, Beijing, China, July 6-11, 2014*, pages 2698–2704. IEEE.

Lu, C., Ball, P., Parker-Holder, J., Osborne, M., and Roberts, S. J. (2022). Revisiting design choices in offline model based reinforcement learning. In *International Conference on Learning Representations*.

Lu, X., Stuehmer, J., and Hofmann, K. (2019). Trajectory VAE for multi-modal imitation.

Ozair, S., Li, Y., Razavi, A., Antonoglou, I., van den Oord, A., and Vinyals, O. (2021). Vector quantized models for planning. In Meila, M. and Zhang, T., editors, *Proceedings of the 38th International Conference on Machine Learning, ICML 2021, 18-24 July 2021, Virtual Event*, volume 139 of *Proceedings of Machine Learning Research*, pages 8302–8313. PMLR.

Radford, A., Wu, J., Child, R., Luan, D., Amodei, D., and Sutskever, I. (2019). Language models are unsupervised multitask learners.

Reed, S., Zolna, K., Parisotto, E., Colmenarejo, S. G., Novikov, A., Barth-Maron, G., Gimenez, M., Sulsky, Y., Kay, J., Springenberg, J. T., Eccles, T., Bruce, J., Razavi, A., Edwards, A., Heess, N., Chen, Y., Hadsell, R., Vinyals, O., Bordbar, M., and de Freitas, N. (2022). A generalist agent.

Schmidhuber, J. (2019). Reinforcement learning upside down: Don't predict rewards - just map them to actions. *CoRR*, abs/1912.02875.

Schrittwieser, J., Antonoglou, I., Hubert, T., Simonyan, K., Sifre, L., Schmitt, S., Guez, A., Lockhart, E., Hassabis, D., Graepel, T., et al. (2020). Mastering atari, go, chess and shogi by planning with a learned model. *Nature*, 588(7839):604–609.

Silver, D., Sutton, R. S., and Müller, M. (2008). Sample-based learning and search with permanent and transient memories. In Cohen, W. W., McCallum, A., and Roweis, S. T., editors, *Machine Learning, Proceedings of the Twenty-Fifth International Conference (ICML 2008), Helsinki, Finland, June 5-9, 2008*, volume 307 of *ACM International Conference Proceeding Series*, pages 968–975. ACM.

Stolle, M. and Precup, D. (2002). Learning options in reinforcement learning. In Koenig, S. and Holte, R. C., editors, *Abstraction, Reformulation and Approximation, 5th International Symposium, SARA 2002, Kananaskis, Alberta, Canada, August 2-4, 2002, Proceedings*, volume 2371 of *Lecture Notes in Computer Science*, pages 212–223. Springer.

Sutton, R. S. (1990). Integrated architectures for learning, planning, and reacting based on approximating dynamic programming. In Porter, B. W. and Mooney, R. J., editors, *Machine Learning, Proceedings of the Seventh International Conference on Machine Learning, Austin, Texas, USA, June 21-23, 1990*, pages 216–224. Morgan Kaufmann.

Sutton, R. S., Precup, D., and Singh, S. (1999). Between mdps and semi-mdps: A framework for temporal abstraction in reinforcement learning. *Artif. Intell.*, 112(1-2):181–211.

van den Oord, A., Vinyals, O., and Kavukcuoglu, K. (2017). Neural discrete representation learning. In Guyon, I., von Luxburg, U., Bengio, S., Wallach, H. M., Fergus, R., Vishwanathan, S. V. N., and Garnett, R., editors, *Advances in Neural Information Processing Systems 30: Annual Conference on Neural Information Processing Systems 2017, December 4-9, 2017, Long Beach, CA, USA*, pages 6306–6315.

Vaswani, A., Shazeer, N., Parmar, N., Uszkoreit, J., Jones, L., Gomez, A. N., Kaiser, L., and Polosukhin, I. (2017). Attention is all you need. In Guyon, I., von Luxburg, U., Bengio, S., Wallach, H. M., Fergus, R., Vishwanathan, S. V. N., and Garnett, R., editors, *Advances in Neural Information Processing Systems 30: Annual Conference on Neural Information Processing Systems 2017, December 4-9, 2017, Long Beach, CA, USA*, pages 5998–6008.

Wang, K., Zhao, H., Luo, X., Ren, K., Zhang, W., and Li, D. (2022). Bootstrapped transformer for offline reinforcement learning. *CoRR*, abs/2206.08569.

Wang, L., Fonseca, R., and Tian, Y. (2020). Learning search space partition for black-box optimization using monte carlo tree search. In Larochelle, H., Ranzato, M., Hadsell, R., Balcan, M., and Lin, H., editors, *Advances in Neural Information Processing Systems 33: Annual Conference on Neural Information Processing Systems 2020, NeurIPS 2020, December 6-12, 2020, virtual*.

Wang, T. and Ba, J. (2020). Exploring model-based planning with policy networks. In *8th International Conference on Learning Representations, ICLR 2020, Addis Ababa, Ethiopia, April 26-30, 2020*. OpenReview.net.

Yang, K., Zhang, T., Cummins, C., Cui, B., Steiner, B., Wang, L., Gonzalez, J. E., Klein, D., and Tian, Y. (2021). Learning space partitions for path planning. In Ranzato, M., Beygelzimer, A., Dauphin, Y. N., Liang, P., and Vaughan, J. W., editors, *Advances in Neural Information Processing Systems 34: Annual Conference on Neural Information Processing Systems 2021, NeurIPS 2021, December 6-14, 2021, virtual*, pages 378–391.

Yu, T., Thomas, G., Yu, L., Ermon, S., Zou, J. Y., Levine, S., Finn, C., and Ma, T. (2020). MOPO: model-based offline policy optimization. In Larochelle, H., Ranzato, M., Hadsell, R., Balcan, M., and Lin, H., editors, *Advances in Neural Information Processing Systems 33: Annual Conference on Neural Information Processing Systems 2020, NeurIPS 2020, December 6-12, 2020, virtual*.

Zheng, Q., Zhang, A., and Grover, A. (2022). Online decision transformer. *CoRR*, abs/2202.05607.

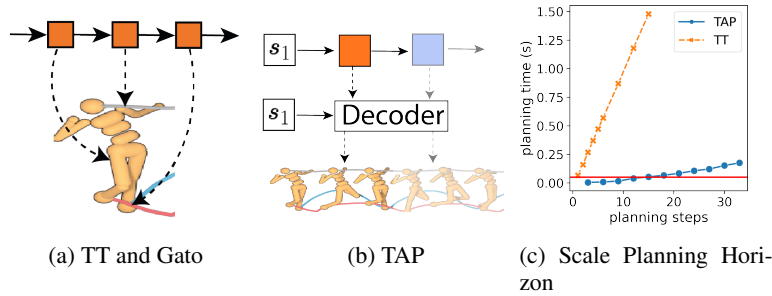|		
(a) TT and Gato	(b) TAP	(c) Scale Planning Horizon

Figure 5: (a) Illustration of dimension-wise autoregressive modelling used by Trajectory Transformer. Blocks represent discretised state/action dimensions or discrete latent variables. (b) shows TAP style modelling. (c) Horizon Scalability, tested for a low-dimensional task, hopper.

A   Scale Up the Planning Horizon

TAP not only makes it easier to scale up the state and action dimensionality, but also helps the agent to plan over a longer horizon with much less computation. As shown in Figure 5(c), the decision latency increases with the number of planning steps, tested on the hopper-medium-replay task. TAP is able to plan 33 steps into the future within 0.25 seconds. Table 3 shows how the performance on locomotion control tasks varies with the planning horizon. We can see that even just expanding a single latent variable (corresponding to 3 steps in the original space), TAP can actually achieve decent performance in most tasks. The longer horizon planning is helpful for hopper, especially in medium-replay settings. In hopper tasks, the agent can easily fall over compared to other tasks. Once the agent falls over, the episode will be immediately terminated, so similar actions might lead to drastic longer-term differences. This might mean learning the dynamics function and using it to help learn the value function is easier than directly learning the value function. On the other hand, the medium-replay dataset has a higher diversity which may make longer planning useful. Both medium and medium expert datasets are generated by one or two fixed policies, this means the possible actions for the next step are quite limited, so searching may not give very different results given the estimated return. The medium-replay dataset, on the other hand, contains the data in the replay buffer. Given the policy parameters are changing during learning, the behaviour policy is then a mixture of a lot of different policies, making TAP has to consider more options when acting.

Table 3: Locomotion performance with different planning horizon

Dataset	Environment	Horizon=3	Horizon=9	Horizon=15	Horizon=21
Medium-Expert	HalfCheetah	91.74	91.17	91.77	90.6
Medium-Expert	Hopper	88.3	104.01	105.53	96.4
Medium-Expert	Walker2d	99.4	107.25	107.44	108.82
Medium-Expert	Ant	126.07	130.96	128.82	134.47
Medium	HalfCheetah	44.01	44.98	45.04	44.7
Medium	Hopper	49.7	64.44	63.44	66.7
Medium	Walker2d	65.04	63.21	64.87	52.03
Medium	Ant	87.8	84.36	92.0	89.87
Medium-Replay	HalfCheetah	40.59	41.51	40.78	41.36
Medium-Replay	Hopper	29.39	90.17	87.3	96.35
Medium-Replay	Walker2d	57.58	58.41	66.85	69.25
Medium-Replay	Ant	83.06	98.67	96.71	97.7
Mean		71.9	81.6	82.5	82.4

B   The Role of OOD Penalty

Besides sampling from the prior distribution given by the transformer, we also used the estimated prior probability to prevent out-of-distribution (OOD) trajectories to be selected during the planning.

15

In Table 4 we showed how the threshold of OOD penalty will affect the performance of TAP. We can see when a very low threshold is chosen $\beta = 10^{-5}$, the performance of the agent drops significantly because the trajectory of such low prior probability will be not sampled in the first place and the OOD penalty is not working. Some of the OOD trajectories with high prediction error and high value will be selected in this case. A larger β in the range of $[0.002, 0.1]$ gives consistent similar results. However, keeping improving β to 0.5 damages the performance again as most of the trajectories do not have such a high prior probability and the penalty will force the agent to choose the most probable trajectory. This $\beta = 0.5$ case can also be treated as an imitation learning baseline, showing searching for the higher return trajectory rather than cloning the behaviour policy is helpful.

Table 4: Locomotion performance with different probability threshold β

Dataset	Environment	$\beta = 10^{-5}$	$\beta = 0.002$	$\beta = 0.01$	$\beta = 0.05$	$\beta = 0.1$	$\beta = 0.5$
Medium-Expert	HalfCheetah	64.3	91.0	90.3	91.8	92.2	87.7
Medium-Expert	Hopper	66.3	95.1	94.5	105.5	107.0	76.1
Medium-Expert	Walker2d	86.6	110.1	109.2	107.4	106.5	104.0
Medium-Expert	Ant	104.7	132.1	133.7	128.8	127.4	116.2
Medium	HalfCheetah	42.6	44.8	44.8	45.0	45.1	42.9
Medium	Hopper	42.9	64.6	67.0	63.4	63.8	47.5
Medium	Walker2d	63.4	49.2	53.8	64.9	64.4	58.7
Medium	Ant	85.1	88.5	89.8	92.0	89.7	85.1
Medium-Replay	HalfCheetah	36.2	42.2	40.5	40.8	40.6	41.0
Medium-Replay	Hopper	19.9	94.4	93.2	87.3	97.0	3.0
Medium-Replay	Walker2d	27.1	57.3	59.6	66.8	65.6	50.3
Medium-Replay	Ant	52.5	96.8	95.7	96.7	93.7	76.8
Mean		57.6	80.5	81.0	82.5	82.8	65.8

C Baselines

As for the baselines, we gather the strong baselines for each of the three sets of tasks. We include model-based methods such as MOReL (Kidambi et al., 2020) and (Optimized) MOPO (Yu et al., 2020; Lu et al., 2022); actor-critic methods CQL (Kumar et al., 2020) and IQL (Kostrikov et al., 2022); and sequence modelling methods DT and TT. We use scores reported by the papers by default with a few exceptions.

- All the methods besides TT did not report performance on Ant locomotion control so we run them using their official codebase.

- For AntMaze-Ultra, we run IQL with their official codebase and run $TT_{(+Q)}$ with the code given by the author (Janner et al., 2021).

- The Ant locomotion results of TT come from their official GitHub repository [3].

- Since CQL is tested in the v0 version of locomotion control tasks, we use the v2 results reported by IQL (Kostrikov et al., 2022).

- All the behaviour cloning (BC) results are reported by D4RL (Fu et al., 2020).

- Chen et al. (2021a, DT) did not report the results for AntMaze and Adroit so we use DT AntMaze results reported by IQL (Kostrikov et al., 2022).

- MOPO results for Adroit come from (Lu et al., 2022).

- TT results for adroit come from (Wang et al., 2022). We also tested two training seeds, each 10 evaluation episodes, for pen-human and pen-cloned and get $12.9_{\pm9.2}$ and $17.3_{\pm9.5}$ respectively.

---

[3]https://github.com/JannerM/trajectory-transformer

D Other Design Potentials for the Bottleneck

The design of the prior model is highly conditioned on the design of the bottleneck and the decoder, and will have an impact when used for planning. Following Decision Transformer (Chen et al., 2021a) and Trajectory Transformer (Janner et al., 2021), we used a GPT-2 style transformer with causal masking for our encoder and decoder. In this case, the information in the future token will not follow back to recent ones. For example, one could reverse the order of the masking for the decoder and make the planning be goal-oriented, whereas the prior should also be trained in a reversed order. In this work, we stick to this particular design and leave others for future work.

We also tried using attention rather than pooling and tiling to construct the bottleneck. Such a design drops the temporal structure of the latent variables, which shows a similar performance when doing vanilla sampling but it prevents using of the beam search so is less efficient.

E AntMaze Details

AntMaze is a sparse-reward continuous-control task in which the agent has to control a robotic ant to navigate to the target position. We include the goal position in the observation space so that the generated trajectories are goal-aware.[4] In order to extensively test different methods, we also add a customized larger antmaze that we called Antmaze-Ultra, which has doubled the size of the previously largest map (Antmaze-Large).

Antmaze has the same dimensionality as locomotion ant and so will not provide too much direct evidence about the action dimension scalability, so it's more about an orthogonal evaluation on sparse reward problems. AntMaze is challenging because there are a lot of sub-optimal trajectories in the dataset that is navigating to different goal positions rather than the target position in the test time. Reaching these goals will not give a reward to the agent. The reward will only be given when the agent reaches the true target, which is also the goal in the test time. On AntMaze, TAP shows better performance on a more challenging large dataset, but is slightly inferior to $\text{TT}_{(+Q)}$ on the medium datasets. We did not use the IQL critic as our value estimator; a better value estimation approach than our current Monte-Carlo estimation would be expected to bring orthogonal improvements. Effective performance without a separate Q-function is partially due to the inclusion of the goal position into the observation: TAP can learn to generalize across goal positions instead of completely relying on the value estimation.

TT has shown using a separate IQL value function can help sequence generative models to solve AntMaze. Such an approach, however, further increases the computational cost for sampling trajectories. Here we instead propose an alternative efficient approach that let TAP jointly leverage trajectories with different objectives and also the reward signals. This is as simple as putting the goal positions to the observation of the agent. We hypothesized that goal positions can be helpful for TAP as it models the whole distribution of the trajectories. When acting in the environment, having the Trajectories conditioned on the goal can narrow down the sampled trajectories to focus on the correct direction, therefore simplifying the planning. Note that for actor-critic methods, the positions of the test time target position are encoded by the critic network and including the goal position will not provide extra information to the agent.

In order to pressure test IQL, TT_{+Q} and TAP in larger AntMaze environments, we introduced the AntMaze-Ultra task, which has 10×14 blocks of effective size. This is 4 and 2 times as large as AntMaze-Medium (6×6) and AntMaze-Large (7×7) tasks, respectively. A visualisation of these three tasks can be found in Figure 6. In addition to the increased size, the complexity of the walls also results in multiple possible routes to navigate from the bottom left corner to the top right. Similar to the antmaze-medium and antmaze-large tasks, we let the agent run for 1K episodes, each with 1K steps to collect the trajectories. However, we find that such an amount of data is far away from being enough to learn a proper value function, as IQL gives a very poor performance on this task. Using the Monte-Carlo estimation, TAP even suffers more from this issue. We find that planning with beam search, in this case, is even worse than just sampling a random trajectory: with random sampling, TAP gives 22.00 +/- 4.14 on AntMaze-Ultra-Play and 26.00 +/- 4.39 on AntMaze-Ultra-Diverse. However, beam search will decrease its performance to 21.00 +/- 4.07 on Ultra-Play and 22.00 +/- 4.14 on Ultra-Diverse.

---

[4]The goal position is specified by the `infos/goal` field in the d4rl dataset by default.

Table 5: Antmaze results. The Antmaze-Ultra is our customised larger environment.

Dataset	Environment	BC	CQL	IQL	DT	$\text{TT}_{(+Q)}$	$\text{TAP}_{(+G)}$
Play	Antmaze-Medium	0.0	61.2	71.2	0.0	**93.3** ±6.4	78.0 ±4.14
Diverse	Antmaze-Medium	0.0	53.7	70.0	0.0	**100.0** ±0.0	85.0 ±3.57
Play	Antmaze-Large	0.0	15.8	39.6	0.0	66.7 ±12.2	**74.0** ±4.39
Diverse	Antmaze-Large	0.0	14.9	47.5	0.0	60.0 ±12.7	**82.0** ±5.00
Play	Antmaze-Ultra	—	—	8.3	—	20.0 ±10.0	**22.0** ±4.1
Diverse	Antmaze-Ultra	—	—	15.6	—	**33.3** ±12.2	26.0 ±4.4
	Mean	-	-	42.0	-	**62.2**	**61.2**

(a) AntMaze-Medium
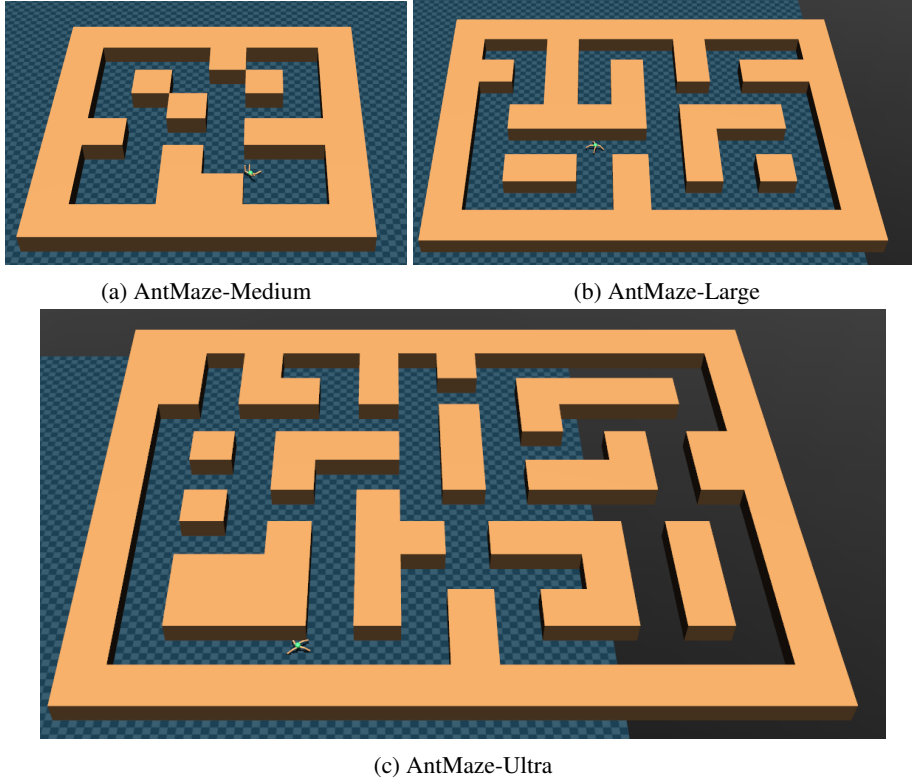

(b) AntMaze-Large

(c) AntMaze-Ultra

Figure 6: Caption

F   Hyperparameters

In Table 6 we showed the hyperparameters for TAP, both for training and planning.

G   Training Cost

The training time of TAP and TT are similar for lower dimensionality, TT needs 6-12 hours and TAP needs 6 hours for gym locomotion control tasks, on a single GPU. It's worth noting that the training cost of TT will also grow quickly along the dimensionality. For adroit, the same training for TT takes 31 hours, but the training cost of TAP is the same given the same architecture. In fact, for adroit experiments with TAP, we used a smaller network (see Table 6 for hyper-parameters) which needs fewer training epochs and the whole training can be finished within 1 hour.

Table 6: List of Hyper-parameters

Environment	Hyper-parameters	Value
All	learning rate	$2e^{-4}$
All	batch size	512
All	dropout probability	0.1
All	number of attention heads	4
All	number of steps for a latent code	3
All	beam expansion factor	4
All	Embedding size for a latent code	512
All	β	0.05
Locomotion Control	training sequence length	24
Locomotion Control	discount	0.99
Locomotion Control	number of layers	4
Locomotion Control	feature vector size	512
Locomotion Control	K	512
Locomotion Control	beam width	64
Locomotion Control	planning horizon	15
AntMaze	training sequence length	15
AntMaze	discount	0.998
AntMaze	number of layers	4
AntMaze	feature vector size	512
AntMaze	K	8192
AntMaze	beam width	2
AntMaze	planning horizon	15
Adroit	training sequence length	24
Adroit	discount	0.99
Adroit	number of layers	3
Adroit	feature vector size	256
Adroit	K	512
Adroit	beam width	256
Adroit	planning horizon	24

Table 7: The ablation of number of steps for a latent code L.

Dataset	Environment	$L=1$	$L=2$	$L=3$	$L=4$
Medium-Expert	HalfCheetah	37.4	68.1	91.8	92.5
Medium-Expert	Hopper	44.7	55.6	105.5	102.2
Medium-Expert	Walker2d	94.9	108.9	107.4	108.5
Medium-Expert	Ant	122.7	118.0	128.8	132.2
Medium	HalfCheetah	43.5	42.6	45.0	45.4
Medium	Hopper	55.1	70.5	63.4	70.7
Medium	Walker2d	35.2	70.6	64.9	69.3
Medium	Ant	92.3	98.2	92.0	88.9
Medium-Replay	HalfCheetah	30.3	30.1	40.8	40.0
Medium-Replay	Hopper	61.9	69.9	87.3	85.6
Medium-Replay	Walker2d	29.4	60.5	66.8	54.8
Medium-Replay	Ant	80.1	90.0	96.7	95.1
Mean		60.6	73.6	82.5	82.1